Research Article

Influence of BFRP Mesh on UHPC Wet Bonding Performance

Yushi Yin [1,2,3] **Min Zhang,**[4] **and Guan-hua Zhang**[3]

[1]*College of Architectural Engineering, Yangzhou Polytechnic Institute, Yangzhou 225127, Jiangsu, China*
[2]*Department of Civil Engineering, Tongji University, Shanghai 200092, China*
[3]*Liaoning Provincial Transportation Planning and Design Institute Co Ltd., Shenyang 110166, Liaoning, China*
[4]*Business School, Yangzhou Polytechnic Institute, Yangzhou 225127, Jiangsu, China*

Correspondence should be addressed to Yushi Yin; yys00080568@163.com

As an effective method of strengthening concrete in the marine environment, wet bonding has maintained an efficient application mode for many years. At present, research on the wet bonding behavior of UHPC is very rare, so in order to investigate the interfacial bonding performance between basalt fiber-reinforced plastic (BFRP) mesh cloth and ultra-high performance concrete (UHPC) under wet bonding conditions, forty-eight BFRP-UHPC specimens were carried out to investigate the influence of dry/wet bonding type, mesh depth, and mesh thickness on the interfacial bonding performance between BFRP and UHPC, and the failure mechanism of the BFRP-UHPC interface was revealed by SEM detection. The test results show that the interfacial wet bonding performance between BFRP and UHPC is better than that of the dry bonding process. With the increasing thickness of BFRP mesh, the interfacial bonding stress of dry and wet bonding shows the opposite trend, respectively. The fiber interlayer structure is the weak link of BFRP; with the increase in mesh depth, the bonding normal stress decreases gradually. When the mesh depth of wet-bonded BFRP is 5 mm, the reinforcement effect is the best, the maximum increase of interfacial bonding stress is 74%, and the tensile strength ratio is as high as 1.74. Compared with the traditional FRP reinforced construction without fiber mesh, the BFRP mesh structure can greatly improve the wet bonding performance, which can provide a theoretical and experimental basis for the design and construction of UHPC wet bonded with BFRP reinforcement engineering. Due to the form and distribution direction of steel fiber, a mechanical occluding effect will be generated at the BFRP mesh, so these two factors are very valuable for this wet bonding research field, for which the related work needs to further proceed.

1. Introduction

Basalt fiber-reinforced plastic (BFRP) has good performance in strength, durability, wet and heat ageing resistance, as well as high temperature resistance. Besides, the mechanical properties and stability of BFRP after exposure to an extreme environment are similar to those of carbon fiber-reinforced plastic (CFRP) cloth [1–3]. However, because of its low price and significantly better performance than glass fiber-reinforced plastic (GFRP) cloth and aramid-fiber reinforced plastic (AFRP) cloth [4, 5], BFRP, as a composite sheet material for reinforced concrete beams and piers, has attracted increasing attention from researchers around the world for its outstanding performance.

The bonding methods for strengthening BFRP beams under the humidity effect can be divided into the dry-bonded method (hereinafter referred to as DEBR) and the wet-bonded method (hereinafter referred to as WEBR) [6–10]. WEBR is often used in FRP composite beams; it refers to the interface formed by pouring concrete when a layer of bonding agent is brushed on the surface of an FRP sheet and the bonding agent starts to stick but has not yet solidified. While, DEBR is to directly coat the bonding agent on the surface of the reinforced concrete substrate and then attach the FRP mesh sheet/plate on it to form a composite structure. In the 1990s, DEBR was the major method for strengthening. However, due to the frequent occurrence of FRP debonding from concrete and the low availability of

FRP sheets, other suitable methods were explored by researchers [11, 12]. In the WEBR method, the wet-bonded strength is 0.50–0.67 times the dry-bonded strength [13]. As the bonding performance of the FRP-concrete interface directly determines the strengthening effect of the concrete beam and as the prestressed FRP technology has become more mature in recent years, the extensive development of the WEBR method has been limited [14–20]. Recently, a large number of composite civil structures, as well as many hydraulic and marine concrete structures, are being built. Although the WEBR method improves the strengthened interface bonding property to a lesser extent than the DEBR method, it is the most practical interface bonding method due to the actual application of newly built composite structures. Based on the demands of offshore, coastal, and marine building construction, further development of wet-bonded technology is of practical significance.

The WEBR strengthening method was first developed by Deskovic et al. [21], and it was found that the composite beam formed in the wet-bonded interface was also subject to stripping damage. Subsequently, Canning et al. [22] compared the bonding effects of six interfaces based on the bending test of an FRP section-concrete composite beam. The results showed that the effect of a wet-bonded interface with epoxy resin was slightly poorer than that of dry bonding. Zhang et al. [10] conducted wet-bonded shear tests of FRP boards and found that the bonding strength of the wet-bonded interface was 1/2–2/3 of the dry bonding strength. Hulatt et al. [14] found that the wet bonding technology was one of the most practical technologies. They reported that when the FRP sheet with incompletely cured glue was attached to the in situ cast beam, the concrete and glue started the chemical curing process simultaneously. Choi et al. [23] applied a thin layer of epoxy glue on the FRP cloth surface first, and then, they laid some coarse or fine aggregates. Then, they determined the bonding strength, fracture energy, and other FRP-concrete interface indexes by studying the interface bonding performance through a single shear test. Huang et al. [24] found that the glue type and the duration of the FRP attached to the cast-in-situ beam surface were two important factors for the interface wet-bonded stress based on the concrete-FRP single shear test. A self-made roughened carbon fiber-reinforced polymer sheet was externally attached to the surface layer of a nano-kaolin-modified concrete test piece to form an RFRP-concrete wet-bonded test piece by Yin et al. [16]; roughened carbon fiber effectively enhanced the wet adhesion performance of the interface with concrete in both normal and tangential directions. Anne et al. [25] investigated the bond strength between concrete and FRP wet lay-up systems using resins with bio-based content of various proportions as a partial replacement of epoxy and found that bond strength was not only dependent on resin but also on fiber type. In the case of glass FRP, bond strengths were generally lower than those of carbon FRPs by 12%–29% for the same resin type. Wang et al. [26] studied the behavior of the FRP-to-concrete interface degraded after salt solution wet-dry cycles and found the debonding load was derived based on the degradation of the FRP-to-concrete interface, the stiffness of the FRP-to-concrete interface degraded obviously, and the durability of the BFRP-to-concrete interface was weaker than that of CFRP. Zhang et al. [5] presented an experimental study on the bond behavior between GFRP plates and concrete under the coupled effects of sustained load and seawater immersion. He found that the ultimate load of the wet bond interface was significantly greater than that of the other three types of interfaces under different coupled-effect ages, and the dry-bonded interface capacity was the worst.

It can be seen from the above research that extensive and systematic research has been carried out on the wet bonding performance between the new and old concrete interfaces in the world. The world's coastline is very long, and there are also many inland lakes, so where concrete structures are built in that environment. Therefore, the treatment of the UHPC wet bonding process is of great engineering significance. At present, few research reports have been found on the reinforcement behavior of UHPC concrete. The safety and reliability of the interfacial bonding between BFRP mesh and UHPC is the basis for ensuring BFRP-UHPC composite constructions. Meanwhile, wet bonding is beneficial to ecological and environmental protection and is very beneficial to the protection of aquatic environments and the rapid construction of underwater concrete. In addition, because it can be prefabricated in the factory, the production cost is greatly reduced, which is of positive significance for production cost control and social life. In this paper, BFRP mesh with the same mesh size is used, and the same UHPC strength grade is used in the same batch of tests. So, the influence of the BFRP production process and concrete strength grade on the interfacial bonding performance is not considered in this paper. By carrying out the tensile bonding test, the three parameters of BFRP dry/wet bonding process type, BFRP mesh thickness, and BFRP mesh anchoring depth are adopted to investigate their influence on the bonding performance of the BFRP-UHPC interface. At the same time, based on the experimental failure phenomenon and statistical analysis of the data, the failure mechanism of the BFRP-UHPC interface is further discussed and revealed.

This project research and technology flowchart is shown in Figure 1. This paper aims to provide a theoretical and experimental basis for UHPC reinforcement design and construction under BFRP wet bonding conditions.

2. Test Scheme

2.1. Test Materials and Properties. The UHPC used in the test was UHPC containing small particle of coarse aggregate, which was composed of cement, silica fume, steel fiber, river sand, stone, water-reducing agent, and water. Cement adopted Changchun Yatai (in China) P∎O52.5 grade ordinary Portland cement; fine aggregate adopted the river sand with a particle size of 1.18–4.75 mm; coarse aggregate adopted the stone with a particle size of 5–10 mm; steel fiber adopted the straight steel fiber produced by Ganzhou Daye Company (80% end hook type and 20% straight wire type, length 13 mm, length diameter ratio 65, tensile strength 2850 MPa); the water reducing agent was the polycarboxylate superplasticizer with a water reducing rate
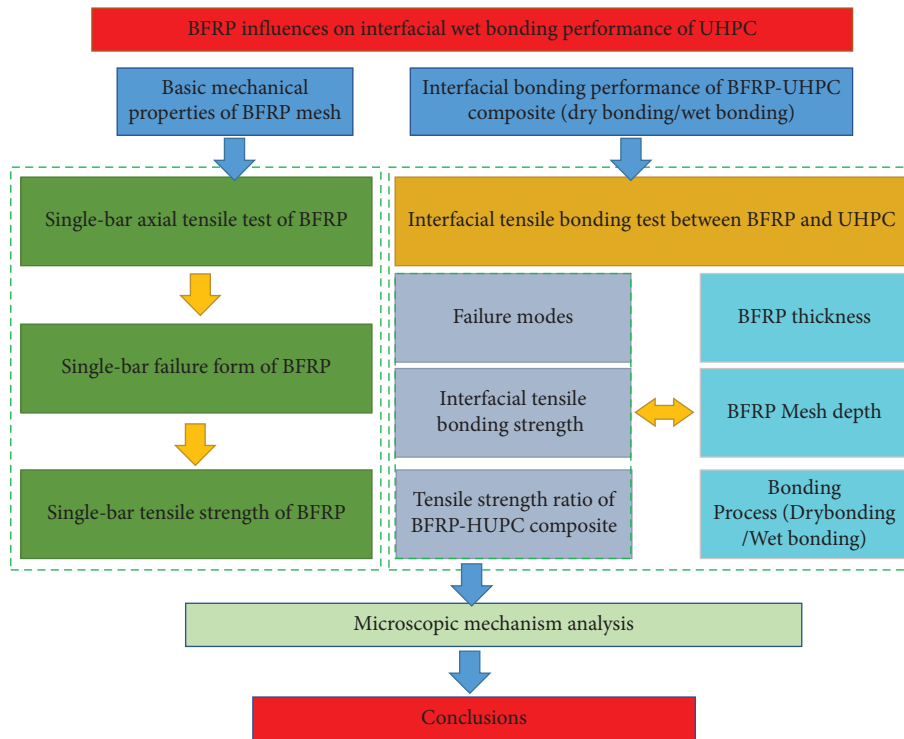
FIGURE 1: Project research technology flowchart.

greater than 30%; silicon powder adopted the microsilicon powder produced by Shanghai Elkem Company. The UHPC composition is shown in Table 1. After 28 days of UHPC mixing and curing, the basic mechanical properties were tested. The compressive strength test of UHPC was carried out according to the code "Standard for inspection and evaluation of concrete strength" (GB/T 50107-2010). The mechanical properties are shown in Table 2. In addition, BFRP adopted the BFRP mesh produced by Yixing Ruibang High-Performance Fiber Products Co., Ltd., with the high temperature laminated product process, with a mesh size of 5 mm × 5 mm, as shown in Figure 1, where its thicknesses were made into 0.85 mm, 1.16 mm, and 1.45 mm, respectively. The interfacial bonding between mesh and UHPC adopted the epoxy resin AB glue produced by the same company and was prepared according to 2:1. The mechanical properties of epoxy resin and steel colloid were tested according to the code "The method for determination of strength properties of adhesive in shear by tension loading" (GB 7124-86)). The BFRP mesh and the steel block were bonded by the steel colloid produced by Zhipan Industrial Co., Ltd., in Shanghai. Other properties of materials are shown in Table 3.

2.2. Single-Bar Axial Tensile Test Scheme of BFRP.

First, in order to examine the tension of the single bar, the mesh was cut into the form of a single bar with a scissor. Then, a layer of epoxy resin glue was lightly applied on the surface of the BFRP. Finally, the epoxy resin was completely cured for 7 days, followed by an ensile failure morphology and tensile performance analysis of a single bar. In the test, a single bar

was pre-stretched before loading to obtain the maximum failure load. Then, a single bar was refixed on the tensile testing machine. According to the test standard, "Testing method for tensile of man-made filament yarns" (GB/T 14344-2008) [27]. The test used 10% of the failure load as the pretension to tension the single bar, and then gradually started tensioning at a loading speed of 1 mm/min to obtain the failure load of the single bar and calculate the tensile strength. In the test, parallel experiments were carried out with 3 pieces/groups, a total of 2 groups.

2.3. Tensile Bonding Test Scheme of BFRP-UHPC.

According to the needs of the fiber tensile bonding test and the technical specification for strengthening concrete structures with carbon fiber sheet reinforced polymer (CECS146-2003) [28], the UHPC samples were made into 48 samples with a size of 70.7 mm × 70.7 mm × 70.7 mm, and the BFRP mesh was coated with 40 mm × 40 mm, with the schematic diagram shown in Figures 2 and 3. Since one of the important parameters investigated in the test is the anchoring depth of BFRP, and in order to greatly weaken the influence of UHPC dispersion, the innovative test method of one body and four sides was adopted in the test; that is, by burying the BFRP mesh with a certain anchoring depth onto two opposite sides of the test piece to conduct the BFRP wet bonding test. In the anchoring operation process of pouring, the pouring height of UHPC was strictly controlled. When the predetermined position of pouring was reached, the BFRP mesh coated with epoxy resin glue (uncured) was immediately laid, and the BFRP mesh was lightly pressed by hand in to make it fully flat contact with the UHPC cement

TABLE 1: UHPC mix proportion (relative mass ratio).

Portland cement	Silica fume	Water	Water reducer	Steel fiber	Fine sand	Crushed stone	W/C
1	0.225	0.225	0.017	0.177	0.900	0.225	0.184

TABLE 2: Mechanical properties of UHPC.

Items	Compressive strength (MPa)	Elastic modulus (GPa)	Initial crack strength (MPa)
UHPC	136	40.2	8.3

substrate, as shown in Figure 4. After that, the pouring continued to complete the test piece.

When the UHPC was completely in the mold, the vibrating table was turned on to vibrate for 20 seconds, then the surface was scraped using a spatula and placed at room temperature (22°C, humidity 30%) for 24 hours before demoulding. It was then put in a curing room for standard curing (20 ± 1°C, humidity ≧ 95%), and could be taken out after 28 days. According to the technical specification for strengthening concrete structure with carbon fiber sheet reinforced polymer [28], the tensile surface was further bonded with steel blocks for the subsequent tensile bonding test. Figure 5 shows the BFRP-UHPC tensile composite test specimens to be performed. When the specimens were ready, they were placed into the pull-out tester, and the BFRP mesh was separated from the UHPC surface layer by the tester to conduct the tensile bonding test process.

2.4. Data Collection and Processing. The tensile performance test of BFRP mesh with a single bar was carried out in parallel with 3 pieces/group, a total of 2 groups. In the test, the failure load was collected, and the tensile strength of the three thicknesses was obtained according to the failure load divided by the cross-sectional area of the single bar. Three tensile strength values were obtained in the test. When the three strength values exceed the average value ± 10%, they should be eliminated and then averaged, with the average value being the final tensile strength value of the single bar.

The tensile bonding test of the BFRP-UHPC interface was carried out in parallel with the results of 6 tests as a group. In the test, the tensile bond strength was obtained by dividing the failure load by the tensile area (bonding area of the bonded steel block). If one of the 6 bond strength values exceeds the average ± 10%, the arithmetic average of the remaining 5 values shall be used as the final result after being eliminated. If any of the 5 values exceeds the average ± 10%, this group of samples is invalid.

3. Test Results and Discussion

3.1. Failure Mode of the Specimens. From the perspective of the test failure process, regardless of the type of dry or wet bonding, the anchoring depth of BFRP, and the thickness of BFRP mesh, and regardless of single-bar tensile or interface tensile bonding tests, all specimens were destroyed instantaneously, and there were no signs of failure. This shows brittle failure characteristics.

3.1.1. Single-Bar Axial Tensile Test Analysis of BFRP. A 10% failure load was applied to the BFRP single bar as preload to keep the bar tightened. Later, as the loading increased gradually, the fibers became increasingly tight, and no obvious sound was heard at this time. When the loading reached about 70%–80% of the failure load, it was observed that smaller fiber filaments broke away from the main bundle of the single bar; when the load reached the failure load, the single bar was snapped and the test was terminated. Observing the cross-section of the single-bar fracture, it was found that the fracture position was generally in the middle of the single bar's two chucks, but the specific failure position was random each time, which is probably due to the uniformity of the BFRP material.

3.1.2. Tensile Test Failure Mode Analysis of Dry Bonding on BFRP-UHPC. The tensile bonding test of BFRP-UHPC was carried out, as shown in Figure 6. In the test, the failure time when the specimens were destroyed was collected. Generally speaking, the failure time of dry bonding was shorter than that of wet bonding. After the destruction, the destruction stage of the BFRP-UHPC interface was observed, as shown in Figure 7. It can be seen that the UHPC interface was basically not damaged, and the interface damage was that the adhesive layer was pulled off so that the BFRP was peeled off from the UHPC surface. As the thickness of the BFRP mesh increased, the volume rate of colloid bonding increased gradually, the failure process became more difficult, and the failure time was gradually prolonged.

3.1.3. Tensile Test Failure Mode Analysis of Wet Bonding on BFRP-UHPC. In order to investigate the influence of BFRP thickness and anchoring depth on the wet bonding performance of the BFRP-UHPC interface, a tensile bonding test of the BFRP-UHPC composite was carried out, and the interface failure morphology was observed, as shown in Figure 8. In the figure, a-b represent the thickness gradient and anchoring depth of BFRP. For example, 2–15 means that the mesh with a thickness of 1.16 mm has an anchoring depth of 15 mm.

In the wet bonding process, after the tensile failure of the BFRP-UHPC sample, there were four failure modes, as shown in Figure 9. When the anchoring depth of the BFRP mesh was 20 mm, the failure modes were I and II, which manifested as flat peeling of the surface of the bonded steel block and UHPC or with a very small amount of mortar,

TABLE 3: Performance parameters of other materials.

Items	Tensile strength (MPa)	Thickness $t1$, $t2$, $t3$ (mm)	Weight (g/m^2)	Mesh size (mm^2)	Elastic modulus (MPa)	Elongation (%)	Shear stress (MPa)
BFRP	1848/2887/5377	0.85/1.16/1.45	200/372/582	5×5	81500/82300/83100	2.76/2.88/2.97	
Epoxy resin	38				2.4×10^3		24.3
Steel colloid	30				1.2×10^4		41.8
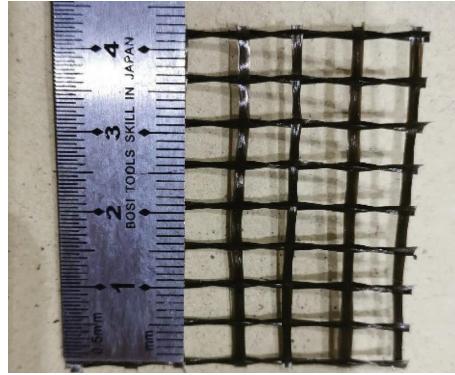
Figure 2: BFRP mesh cloth.
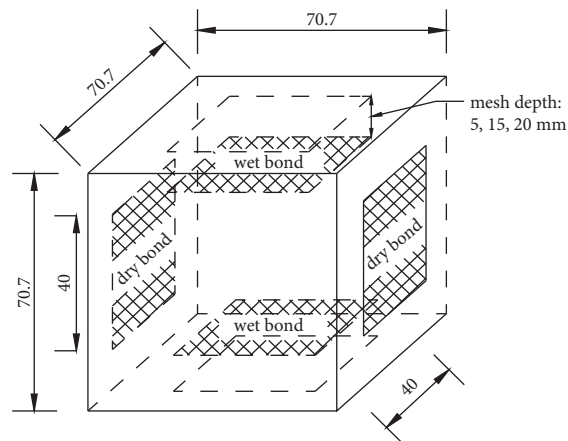
Figure 3: Schematic diagram of the BFRP mesh cloth paste area.

|(a)|(b)|
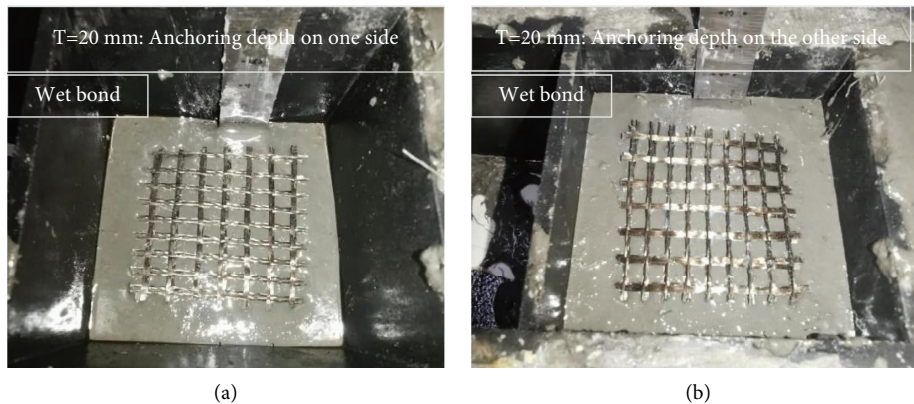
Figure 4: Anchoring depth of wet-bonded BFRP mesh. (a) 20 mm anchoring depth on one side. (b) 20 mm anchoring depth on the other side.

and the bonding effect between the bonded steel glue and the surface layer of UHPC was not good. When the anchoring depth of the BFRP mesh was 5 mm or 15 mm, the failure modes were III and IV, meaning that the bonded steel block would tear off a certain thickness of mortar layer or concrete block from the surface of UHPC, and the bonding effect was better. The reason for the above-mentioned was that when the BFRP mesh was deeply anchored, the adhesive steel directly acted on the UHPC surface, and the stress transfer depth was less than the anchoring depth. In other words, as the anchoring depth gradually increased, the bond failure of the UHPC surface became less obvious; in addition, as the thickness of the BFRP mesh gradually increased, the damage degree of the UHPC surface transitioned from very significant to a slight failure.

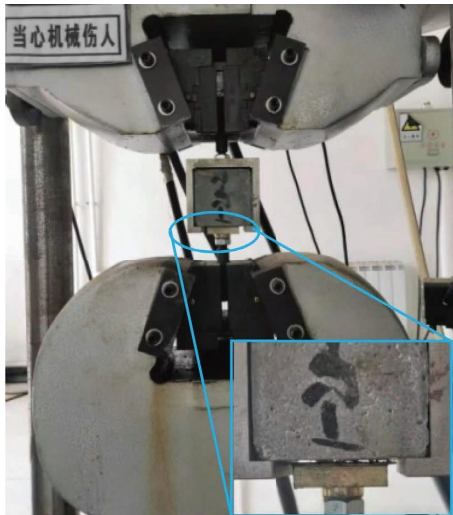Figure 5: BFRP-UHPC tensile bonding test specimens.
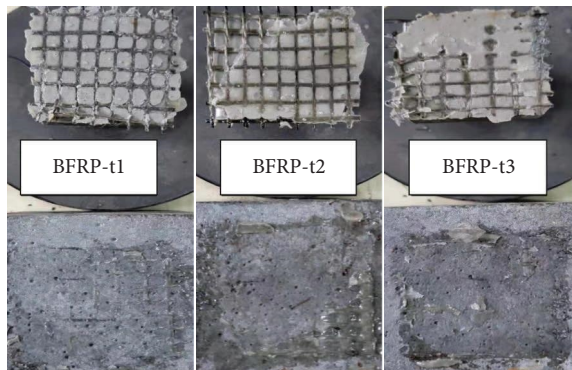

Figure 6: BFRP-UHPC pull-out bond test.

Figure 7: Failure mode of the dry bond in pull-out test of different thicknesses.

From the perspective of the tensile failure mode of BFRP-UHPC wet bonding, with the increase in BFRP anchoring depth, the interface failure degree shows a trend of decreasing gradually. After the interface failure, the surface of the BFRP was accompanied by UHPC surface concrete particles or mortar with uneven thickness. When the BFRP anchoring depth was 15 mm, in addition to the damage in the bonding area, a small piece of UHPC surface concrete
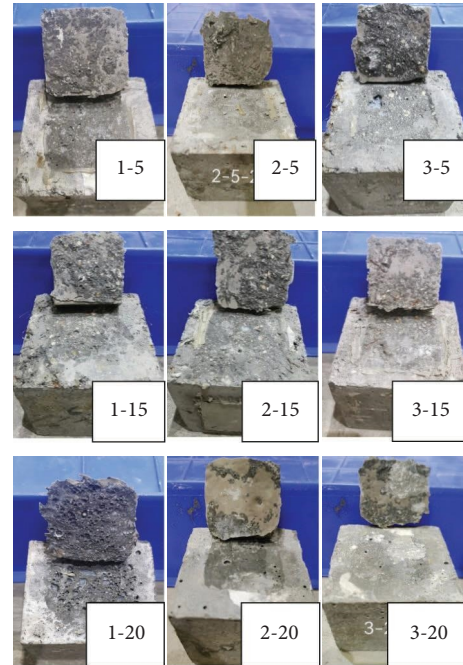

Figure 8: Interface failure performance.

was torn off around the bonding area at the same time. In addition, at the same anchoring depth, with the increase in BFRP mesh thickness, the interface damage degree gradually decreased. It can be considered that in the BFRP wet bonding reinforcement, the BFRP thickness and anchoring depth directly determine the interface failure mode.

3.2. Single-Bar Axial Tensile Strength Analysis of BFRP. Since the tensile process and strength analysis of BFRP mesh with different thicknesses are similar, a mesh with a thickness of 1.45 mm was used as an example for analysis and description. Figures 10 and 11, respectively, show the loading in situ and strain-load relationship curves. It is not difficult to find from the test data that BFRP strictly conformed to elastic deformation failure in tensile failure, and the failure load ranged from 6.315 kN to 7.524 kN. There are three reasons for the dispersion of data under the same parameters. The first and most important reason was that when the epoxy resin glue was manually applied to the surface of BFRP, it could not be strictly accurate to a thin layer, and the test technicians were mostly based on subjective factors in operation, each operation could not be strictly consistent so that the nominal diameter of the BFRP cross-sectional direction could not be consistent after the glue. As a result, the tensile strength test data shows a certain dispersion. The second is the distortion of the BFRP mesh caused by the experimenters' cutting the BFRP single bar. Although the epoxy resin colloid was not applied in this process, internal damage had already occurred, and the damaging effect was still present after the later application of the glue. The third is that the BFRP single bar was not fully subjected to the axial loading on the loader; the loading effect of the first twist could occur before the axial loading
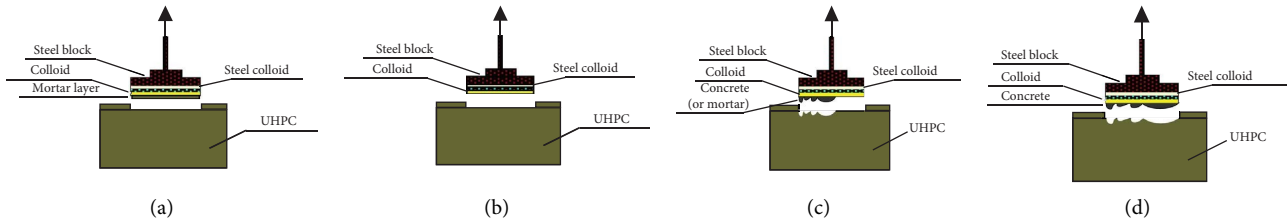
Figure 9: Specimen failure modes: (a) mode I, (b) mode II, (c) mode III, and (d) mode IV.

Figure 10: Axial tension test of a BFRP single bar.

Figure 11: Strain-load relation curve of a BFRP single bar.

occurred. This distortion greatly damaged the cured BFRP single bar and also greatly damaged the tensile strength of the BFRP single bar. Due to the implementation of BFRP single-bar preloading in the test, the first two cases are the main reasons for the data fluctuation.

3.3. Analysis of the Tensile Bond Strength of BFRP-UHPC Interface.
It can be seen from Figure 12 that, under the dry bonding process, with the increase in the thickness of the BFRP mesh, the bonding strength of the BFRP-UHPC interface increased from 4.156 MPa to 4.862 MPa, an increase of 16.97%. This was because when the normal stress was transmitted to the UHPC, as the thickness of the BFRP mesh increased, the elastic modulus of the BFRP increased, and the mechanical tensile strength contributed by the BFRP itself increased, so the interfacial bonding stress increased.

In the wet bonding process, with the increase in thickness of the BFRP mesh, the interfacial bonding strength decreased to varying degrees, and the reduction rates were
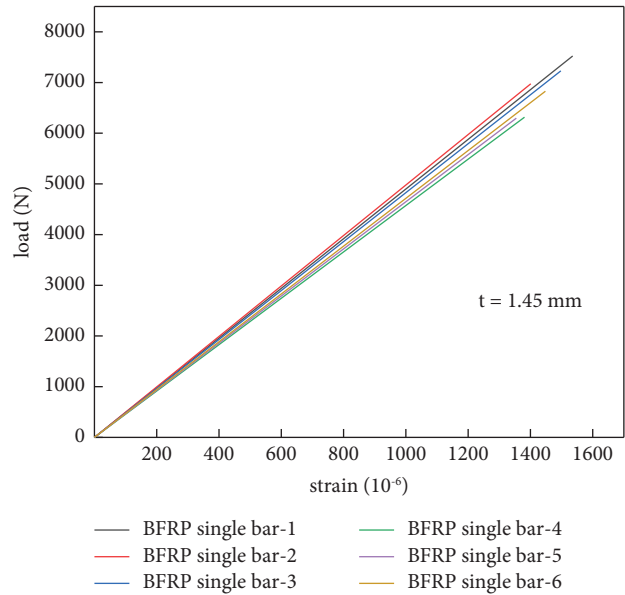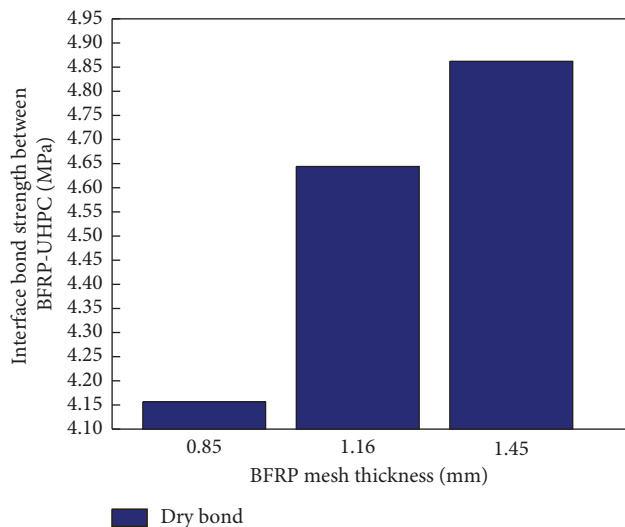

Figure 12: Variation curve of interface bond strength with mesh thickness under a dry bond process.

41.2%, 48.1%, and 38.4%, respectively, as shown in Figure 13. The reason is that in the BFRP process, the standard thickness is 0.85 mm. In order to investigate the influence of BFRP thickness on the bonding performance, the
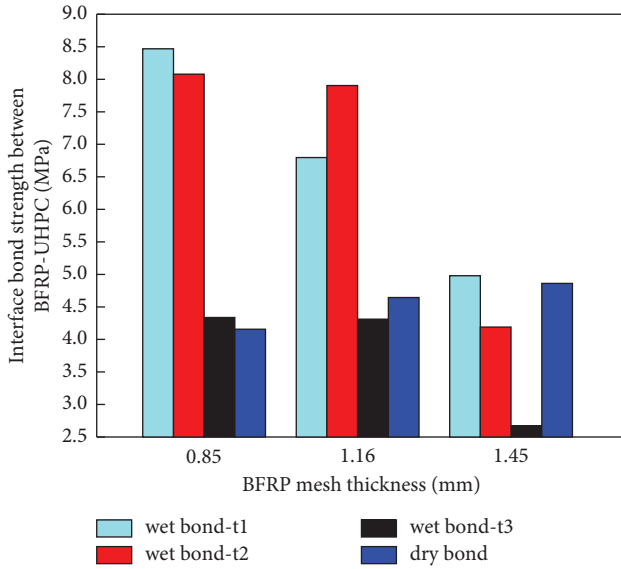
Figure 13: Comparison curve of interfacial bond strength under the dry and wet bond processes.

manufacturers adopt a high temperature lamination process; that is, a layered interface structure appears on the original material. Thus, as the thickness of the mesh increases, the bonding stress is transmitted to the anchoring depth of the BFRP mesh. A part of the thickness of the BFRP mesh cannot provide normal stress, and the interface debonding phenomenon occurs, which will be further explained in the SEM analysis failure mechanism. In addition, generally speaking, the bonding strength of a wet bonding interface is higher than that of a dry-bonding interface. When the anchoring depth of wet bonding was 5 mm, the re-inforcement effect was most obvious, which was 1.08 times higher than that of the dry bonding interface. The reason for the above results was that when the anchoring depth was large, the stress transfer depth of the tensile bond was smaller than the anchoring depth, and the tensile stress was only provided by the tensile strength of the UHPC surface layer. Besides, the tensile strength of the UHPC was less than that of the UHPC-BFRP composite. Therefore, the premature failure of the interface occurred, which was reflected in the small value of the bonding stress. On the contrary, when the BFRP mesh was embedded near the surface layer of UHPC in the BFRP-UHPC composite, the BFRP provided sufficient tensile properties, and the interfacial bonding stress was large.

3.4. Tensile Strength Ratio of BFRP-UHPC Composite.

In order to reflect the contribution of BFRP to the UHPC substrate, the tensile strength ratio was used to investigate the change law of UHPC's tensile bonding stress before and after the BFRP mesh was embedded. The tensile strength ratio is one of the more important parameters of composite materials [29, 30], which is calculated by

$$\xi = \frac{f_{ct,2}}{f_{ct,1}}, \tag{1}$$

where ξ is the tensile strength ratio, dimensionless; $f_{ct,2}$ is the interface tensile strength of wet-bonded BFRP-UHPC, MPa; $f_{ct,1}$ is the interface tensile strength of the dry-bonded BFRP-UHPC, MPa.

As shown in Figure 14, the interfacial bonding strength of dry-bonded UHPC is relatively low. Here, we compare the test conditions with a dry-bonded BFRP mesh with a maximum thickness of 1.45 mm. The tensile strength of the dry-bonded interface is 4.862 MPa, while the bonding performance of the UHPC composites embedded in the BFRP mesh has been greatly improved, with the maximum increase rate reaching 74% and the tensile strength ratio being 1.74, which appeared under the working condition of an anchoring depth of 5 mm. When the thickness of the BFRP mesh changed, in general, the bonding strength of the wet bonding interface was higher than the maximum tensile strength of the dry bonding interface. Therefore, it is certain that the thin-layer BFRP mesh placed in the shallow layer of UHPC has a significant effect on improving the tensile strength of the UHPC interface. The tensile strength ratios of 0.89, 0.88, 0.86, and 0.55 occurred because the minimum tensile strength of wet bonding was compared with the maximum bonding stress of dry bonding, making the tensile strength ratio less than 1. In addition, for the wet bonding process with an anchoring depth of 20 mm, the tensile strength ratio is generally not high due to the weak contribution of the BFRP mesh.

4. Microscopic Mechanism Interpretation of the Wet Bonding Failure of BFRP-UHPC

According to the sampling requirements of the scanning electron microscope (SEM) [31, 32], some samples of BFRP-epoxy resin glue, BFRP-UHPC composite material, and UHPC of 10 mm × 10 mm × 10 mm were collected. The research on the variational regularities of surface micro-structures before and after loading was observed using SEM technology (model of machine SS-550, Shimadzu, Japan).

It is clear from Figures 15 and 16 that epoxy resin colloid plays an important role in protecting BFRP and maintaining its overall performance. During the curing process of the epoxy resin glue on the BFRP mesh, the overall stiffness of the BFRP mesh is further enhanced, and its mechanical properties are improved. In the process of BFRP single bar and BFRP-UHPC tensile bond test, the colloid is stretched and fractured first, then the load is concentrated by the composite material itself, and the BFRP mesh that loses the epoxy resin bonding protecting performance, so the tensile strength of BFRP single bar is low, and it is extremely fractured when the BFRP single bar reaches its failure load. It can be seen from Figure 15 that the multilayer BFRP composite structure has been separated into layers at this time, and the colloid has been immersed in the layered
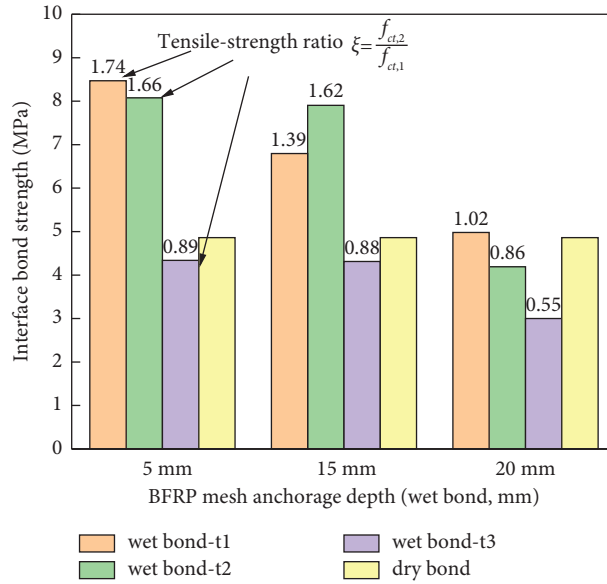
FIGURE 14: Interfacial tensile strength and tensile strength ratio of the BFRP and UHPC specimens.
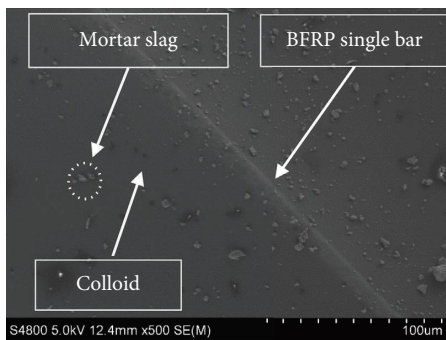

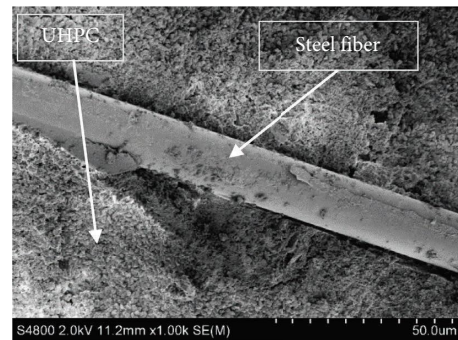FIGURE 15: Morphology of a BFRP filament in colloid.

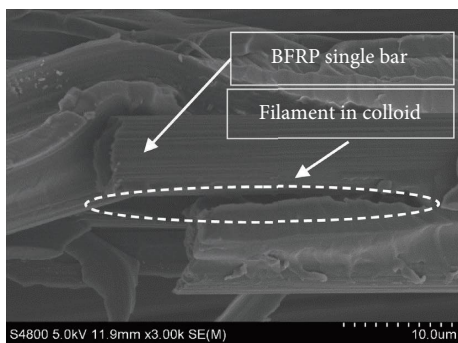FIGURE 17: BFRP fiber link UHPC between separation concrete.

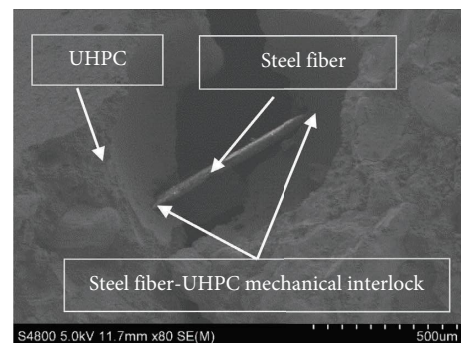FIGURE 16: Debonding of a BFRP filament in colloid.

FIGURE 18: Morphology BFRP fiber in UHPC.

interface. Under the load action, the colloid has been debonded from the BFRP single bar, and the bearing capacity of the BFRP mesh is reduced, resulting in obvious damage, reflecting the material failure process during loading.

Steel fiber plays a role in improving the toughness of UHPC. The steel fibers remain connected after failure, and UHPC has residual stiffness and strength. It can be seen

from Figure 17 that the interface between the steel fiber and the UHPC substrate is well bonded when it is not destroyed completely, while Figure 18 shows that when the tensile stress exceeds the tensile strength of the UHPC, the UHPC is broken and damaged, while the steel fiber is unbroken. There is a certain anchoring interval in the UHPC substrate, along with the corresponding anchoring mechanical properties, so that the UHPC still has its residual stiffness and strength. In

the tensile bonding test, due to the horizontal distribution of the BFRP mesh, the BFRP mesh formed as a whole composite as a function of the epoxy resin, and the steel fibers did not "mechanically interlock" with the BFRP mesh under the vertical bonding stress. Unfortunately, no effect of the steel fibers on the BFRP was observed; this is because the loading method is vertical.

5. Conclusions

Three parameters of BFRP dry/wet bonding process type, BFRP mesh thickness, and BFRP mesh anchoring depth are adopted to invest their influences on the interfacial bonding performance between BFRP and UHPC. At the same time, based on the experimental failure phenomenon and statistical analysis of the data, the failure mechanism of the BFRP-UHPC interface is further discussed and revealed. The following conclusions are drawn:

(1) The wet bonding strength of the BFRP-UHPC interface is higher than that of the dry bonding process. Since BFRP provides sufficient tensile properties, the bonding stress at the BFRP-UHPC interface is large.

(2) With the increasing thickness of BFRP mesh, the interfacial bonding stress of dry and wet bonding and UHPC showed an opposite trend of gradually increasing and decreasing, respectively. The plane interlayer interface is the weak link of BFRP. Even if the epoxy resin is impregnated, under the action of an external load, after the overall structure of the interlayer is damaged, the load-bearing performance of BFRP decreases and accelerates.

(3) With the increase in the anchoring depth of the BFRP mesh, the interfacial bonding stress shows a decreasing trend. When the anchoring depth is 5 mm, the reinforcement effect is the best.

(4) Due to the limitation of the mesh size of BFRP, some coarse aggregates could not pass through the mesh, and objectively, the bonding between the UHPC cement-based gel material and BFRP plays a dominant role. Since most of the coarse aggregates failed to interweave with the BFRP mesh, further improvement of the wet bonding performance was limited. The follow-up work needs to further increase the mesh size of the mesh to investigate the influence of coarse aggregate on the wet bonding performance.

(5) The distribution pattern of steel fibers near the surface of UHPC has a significant effect on the interfacial bonding stress, especially wet bonding. Due to the structural form and distribution direction of steel fiber, mechanical occluding stress will be generated at the BFRP grid, so these two factors are very valuable for research, which is the vacancy of current research, and related work needs to further proceed.

Notation

ξ: The tensile strength ratio (dimensionless)
$f_{ct,2}$: The interfacial tensile strength of wet-bonded BFRP-UHPC (MPa)
$f_{ct,1}$: The interfacial tensile strength of the dry-bonded BFRP-UHPC (MPa)
t: The BFRP mesh thickness (mm)
T: Anchoring depth of wet-bonded BFRP mesh (mm).

Data Availability

The data used to support the findings of this study are available from the corresponding author upon reasonable request.

Conflicts of Interest

The authors declare that they have no conflicts of interest.

Acknowledgments

References

[1] Y. F. Li and Y. Y. Sung, "Seismic repair and rehabilitation of a shear-failure damaged circular bridge column using carbon fiber reinforced plastic jacketing," *Canadian Journal of Civil Engineering*, vol. 30, no. 5, pp. 819–829, 2003.

[2] Y. Ma, L. Gao, and F. Zhang, "Test and numerical simulation of shear strengthening of reinforced concrete T-beam with HU-FRP," *Journal of Building Materials*, vol. 24, no. 05, pp. 1073–1081, 2021.

[3] L. J. Ouyang, W. Y. Gao, B. Zhen, and Z. D. Lu, "Seismic retrofit of square reinforced concrete columns using basalt and carbon fiber-reinforced polymer sheets: a comparative study," *Composite Structures*, vol. 162, pp. 294–307, 2017.

[4] Z. Q. Liu, Z. X Guo, and Y. Ye, "Experimental study on bonding performance of interface between PSWR-PM reinforcement layer and concrete," *Journal of Building Materials*, vol. 2021, Article ID 6676494,12 pages, 2021, https://kns.cnki.net/kcms/detail/31.1764.TU.20210824.1248.008.html.

[5] P. Zhang, Y. Hu, Y. Pang et al., "Experimental study on the bond behavior of GFRP plate-high-strength concrete composite interfaces under the coupled effects of sustained load and seawater immersion," *Structures*, vol. 30, pp. 316–328, 2021.

[6] in*Report on Fiber-Reinforced Polymer (FRP) Reinforcement for concrete Structures*, American Concrete Institute, Michigan, USA, ACI 440R-07 2008, 2008.

[7] L. C. Bank, "Progressive failure and ductility of FRP composites for construction: Review," *Journal of Composites for Construction*, vol. 17, no. 3, pp. 406–419, 2013.

[8] F. S. Chen, G. F. Zhao, and D. Q. Pan, "Test research on rehabilitation with CFRP bonded externally on moist concrete

surface," *Journal of Dalian University of Technolgy*, vol. 48, no. 05, pp. 698–701, 2008.

[9] Y. S. Yin and Y. F. Fan, "Experimental research on the wet bonding properties between RFRP and concrete," *Advances in Structural Engineering*, vol. 23, no. 5, pp. 857–868, 2019.

[10] P. Zhang, D. Y. Gao, and H. Zhu, "Numerical simulation and experimental study on the performance of wet-bonding interface between FRP plate and concrete," *Journal of China Civil Engineering*, vol. 46, no. 02, pp. 108–114, 2013.

[11] L. Li, Y. Shao, and Z. Wu, "Durability of wet bond of hybrid laminates to cast-in-place concrete," *Journal of Composites for Construction*, vol. 14, no. 2, pp. 209–216, 2010.

[12] Y. Shao, Z. S. Wu, and J. Bian, "Wet-bonding between FRP laminates and cast-in-place concrete," in *Proceedings of the International Symposium on Bond Behaviour of FRP in Structures*, pp. 91–96, Hangzhou City, Zhejiang Province, China, 2005.

[13] P. Zhang, *Experimental Research on Mechanical Performance of FRP-concrete Composite Beam*, pp. 29–39, Southeast University, Bangladesh, 2011.

[14] J. Hulatt, L. Hollaway, and A. Thorne, "Short term testing of hybrid T beam made of new p material," *Journal of Composites for Construction*, vol. 7, no. 2, pp. 135–144, 2003.

[15] Z. Wu, W. Li, and N. Sakuma, "Innovative externally bonded FRP/concrete hybrid flexural members," *Composite Structures*, vol. 72, no. 3, pp. 289–300, 2006.

[16] Y. S. Yin, Y. F. Fan, and Y. H. Xu, "Roughness effects on the shear bonding properties of interface between CFRP and concrete," *Journal of Building Materials*, vol. 21, no. 2, pp. 202–207, 2018.

[17] X. Y. Tian, *Mechanical Properties of HFRP and Bonding between HFRP and Casting-In-Place concrete*, Zheng Zhou University, Zhengzhou, China, 2007.

[18] K. H. Cho, J. R. Cho, W. J. Chin, and B. S. Kim, "Bond-slip model for coarse sand coated interface between FRP and concrete from optimization technique," *Computers and Structures*, vol. 84, no. 7, pp. 439–449, 2006.

[19] R. El-Hacha and D. Chen, "Behaviour of hybrid FRP-UHPC beams subjected to static flexural loading," *Composites Part B: Engineering*, vol. 43, no. 2, pp. 582–593, 2012.

[20] P. Feng and X. Lu, *Fiber Reinforced Composite Construction Application Technology Tests, Theory and Methods*, China Building Industry Press, China, 2011.

[21] N. Deskovic, T. C. Triantafillou, and U. Meier, "Innovative design of FRP combined with concrete: short-term behavior," *Journal of Structural Engineering*, vol. 121, no. 7, pp. 1069–1078, 1995.

[22] L. Canning, L. Hollaway, and A. M. Thorne, "An investigation of the composite action of an FRP/concrete prismatic beam," *Construction and Building Materials*, vol. 13, no. 8, pp. 417–426, 1999.

[23] S. Choi, A. L. Gartner, N. V. Etten, H. R. Hamilton, and E. P. Douglas, "Durability of concrete beams externally reinforced with CFRP compo-sites exposed to various environments," *Journal of Composites for Construction*, vol. 16, no. 1, pp. 10–20, 2012.

[24] H. Huang, W. Wang, and F. Zhao, "Experimental study on the bond behavior at the GFRP-concrete interface under wet bonding technique," *Industry Construction*, vol. 43, pp. 192–195, 2013.

[25] A. McIsaac, K. Mak, and A. Fam, "Influence of resin bio-content and type on bond strength between FRP wet layup and concrete," *Journal of Composites for Construction*, vol. 23, no. 4, 2019.

[26] Y. L. Wang, X. Y. Guo, S. Shu, Y. Guo, and X. Qin, "Effect of salt solution wet-dry cycling on the bond behavior of FRP-concrete interface," *Construction and Building Materials*, vol. 254, pp. 119317–120618, 2020.

[27] China National Standardization Administration, *Testing Method for Tensile of Man-Made Filament Yarns*, China National Standardization Administration, China, 2009.

[28] Ministry of Transport of the People's Republic of China, *Technical Specification for Strengthening concrete Structures with Carbon Fiber Sheets (CECS 146:2003)*, People's Communications Press, Beijing, China, 2002.

[29] L. Li, Y. Shao, and Z. Wu, "Durability of wet bond of hybrid laminates to cast-in-place concrete," *Journal of Composites for Construction*, vol. 14, no. 2, pp. 209–216, 2010.

[30] G. Ma and H. Li, "Experimental study of the seismic behavior of pre-damaged reinforced-concrete columns retrofitted with basalt fiber-reinforced polymer," *Journal of Composites for Construction*, vol. 19, no. 6, Article ID 04015016, 2015.

[31] Y. Pan, Q. Liu, and Y. Ren, "Experimental study on bonding performance of CFRP chain concrete interface based on different bonding materials," *Journal of Civil Engineering*, vol. 54, no. 01, pp. 26–37, 2021.

[32] X. M. Ren, *Scanning Electron Microscope/Energy Spectrum Principle and Special Analysis Technology*, Chemical Industry Press, Beijing, 2020.